LIQUID AND SOLID PHASES OF LASER COOLED IONS*

S.L. Gilbert, J.C. Bergquist, J.J. Bollinger,
W.M. Itano, and D.J. Wineland

National Bureau of Standards, Boulder, CO 80303

ABSTRACT

Experiments on collections of strongly coupled laser cooled atomic ions performed at the National Bureau of Standards are summarized. We first discuss strong coupling of small numbers ($\lesssim 20$) of atomic ions confined in a Paul electrodynamic (rf) trap, in which crystalline structures are observed. We then discuss experiments in which shell structure is observed for up to 15 000 ions confined by static electric and magnetic fields. These clouds display liquid and solid-like behavior similar to that of a smectic liquid crystal. Future experiments are suggested, including some where infinite volume behavior may be observable.

1. INTRODUCTION

Strong coupling in collections of charged particles occurs when the Coulomb interaction energy between nearest neighbors is larger than their respective thermal energies. Particles in such a system can display spatial ordering characteristic of liquid and solid phases. Our interest in this field was in part stimulated by a 1977 paper of Malmberg and O'Neil[1] who discussed the possibility of achieving liquid and solid-like behavior in a pure electron plasma confined in a Penning trap. It seemed possible to us that the strong coupling condition could be achieved in a sample of laser cooled ions. Although the conditions for strong coupling have been produced in ions[2,3] and electrons[4] confined in Penning traps, evidence for

spatial ordering was not obtained until recently. In this paper we will discuss the observation of crystalline clusters[5,6] and shell structures[7] in laser cooled, trapped ion clouds.

Strong coupling in Coulomb systems is of interest in several fields of physics and is expected to give rise to a variety of many-body phenomena.[8] In addition to the ion trap work described here, strong coupling has been observed in small numbers ($\lesssim 100$) of macroscopic charged particles confined in a rf trap,[9] 2D configurations of electrons near the surface of liquid helium,[10] and charged particles in liquid suspension which act through a shielded Coulomb potential.[11] Future possibilities for observation include ordering of particles confined in high energy storage rings.[12]

The static thermodynamic properties of an ion cloud confined in a trap are identical to those of a one-component plasma (OCP).[1,8] An OCP consists of a single species of charged particles embedded in a uniform-density background of opposite charge. For the system of ions in a trap, the trapping fields play the role of the neutralizing background charge. An OCP can be characterized by the Coulomb coupling constant,[1,8]

$$\Gamma \equiv q^2/(a_s k_B T), \qquad (1)$$

which is a measure of the nearest neighbor Coulomb energy divided by the thermal energy of a particle. The quantities q and T are the ion charge and temperature. The Wigner-Seitz radius a_s is defined by $4\pi a_s^3 n_0/3 = 1$, where $-qn_0$ is the charge density of the neutralizing background.

An infinitely large OCP is predicted[8] to exhibit liquid-like behavior (short range order) for $\Gamma > 2$ and have a liquid-solid phase transition to a body-centered cubic (bcc) lattice at $\Gamma \cong 178$. In the following sections we will describe work at the National Bureau of Standards (NBS) on strong coupling of atomic ions confined in rf and Penning traps. The spatial ordering observed in these experiments was greatly influenced by the boundary conditions imposed on the

clouds due to the trapping fields. In the last section, we will discuss future experiments in which the infinite volume bcc lattice may be observed.

2. COULOMB "CLUSTERS" IN A RF TRAP (≤ 20 IONS)

With the practical density and charge limitations imposed on atomic ions in electromagnetic traps, very low temperatures must be realized in order to obtain $\Gamma >> 1$. This has been achieved by laser cooling. Here we describe an experiment using Hg^+ ions at NBS.[5] A similar experiment has been performed on Mg^+ ions at the Max Planck Institute for Quantum Optics in Garching.[6]

Small numbers of $^{198}Hg^+$ ions were stored in a miniature rf trap[13] shown schematically in Fig. 1. The trapping potential is provided by the ponderomotive potential, or pseudopotential, resulting from the application of a spatially inhomogeneous, time varying electric field.[14]

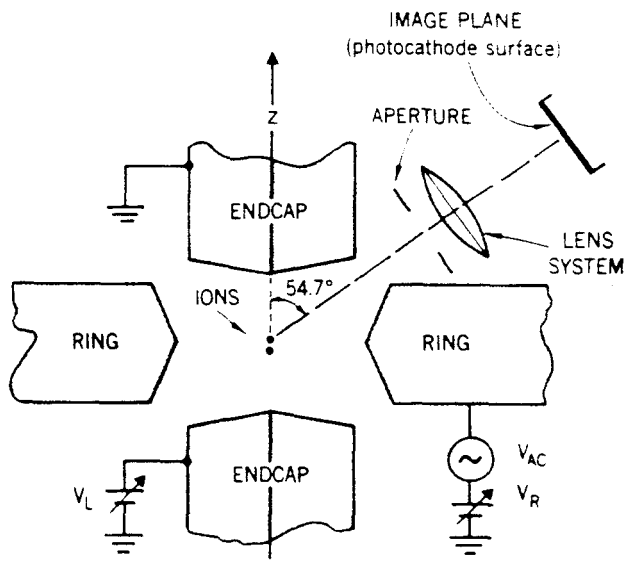

Fig. 1 Schematic drawing of the trap electrodes and imaging system (not to scale) for Hg^+ cluster experiments. The end-cap to end-cap separation along the z axis is approximately 625 μm. The overall magnification of the lens system is 180X. The laser beam used to illuminate the ions enters the trap at an angle of 54.7° with respect to the z axis and is perpendicular to the observation axis.

The ions were laser cooled ($T \leq 8$ mK) by 1-2 μW of cw 194 nm radiation whose beam waist was varied between 5 and 15 μm at the position of the ions. This radiation was tuned near the $5d^{10}6s\ ^2S_{\frac{1}{2}} \rightarrow 5d^{10}6p\ ^2P_{\frac{1}{2}}$ resonance line. Some of the 194 nm fluorescence from the ions was focused onto the photocathode of a resistive-anode photon-counting imaging tube as shown in Fig. 1. The optics for the imaging was provided by a three-stage fused-quartz lens system with an aberration-compensated first stage. The first lens was apertured to give an f number of 4.5. The positions of the photons detected by the imaging tube could be displayed on an oscilloscope in real time or stored by a computer in order to make time exposures.

In Fig. 2a we show the orientation of the trap as viewed by the imaging tube. The remainder of Fig. 2 shows images obtained for various numbers (≤ 16) of ions. Below the images in Figs. 2d through g, are the configurations obtained theoretically[15] by minimizing the energy for each value of the number of ions N_i for a given trapping potential. The rings in Figs. 2e through g are due to ion circulation about the z axis. The number of ions could be assigned by stretching the ions out along the z axis, as in Fig. 2c, or by varying the trapping parameters (V_{AC} and V_R in Fig. 1) and comparing the observed images with the simulations.

Although the trap was designed to have axial symmetry, there is apparently a small asymmetry which caused the ions in 2b to align along the x axis. This pinning also occurred in 2d due to the extra asymmetry of an impurity ion. In the experiments of Ref. 6, the trap asymmetry in the x-y plane was apparently larger than observed here and caused pinning of like ions under a wide variety of conditions.

These clusters of atomic ions can be viewed as pseudomolecules whose optical spectra would be expected to show rovibronic structure. We have measured the mode structure of the diatomic pseudomolecule $(Hg^+)_2$ by probing its optical structure.[5] This was done by measuring the spectrum of the $^2S_{1/2}(m_J = +1/2) \rightarrow {}^2D_{5/2}(m_J = -1/2)$ electric quadrupole transition ($\lambda \cong 282$ nm) of one of these ions and observing the sidebands due to the stretch and rocking motions of the ions.

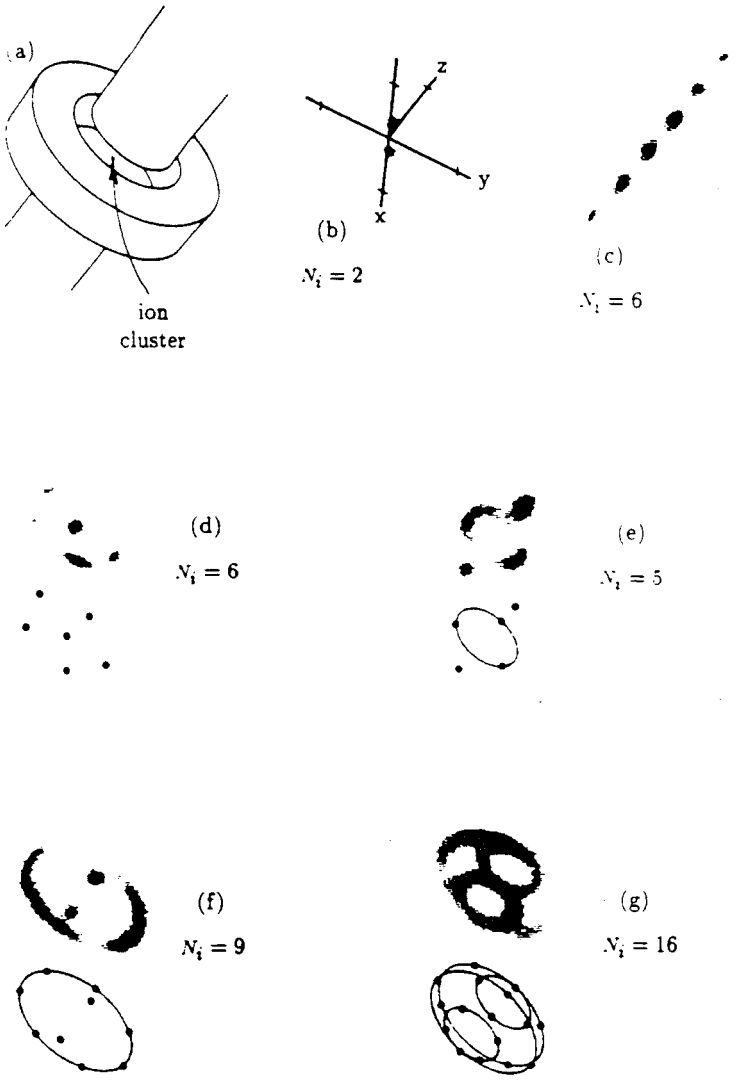

Fig. 2 Images of Hg^+ ion "clusters" in a rf trap. In (a), the trap electrodes are shown schematically in the same orientation as for the remainder of the pictures, but at reduced magnification. The coordinate system in (b) applies to the rest of the images. The ticks on the axes are 10 μm from the origin. In (d) through (g), we display numerical solutions for the expected cluster shapes using the experimental value of the trapping potential. In (d), a nonfluorescing impurity ion occupies one of the ion sites in the cluster and helps pin the ions in the radial plane.

Finally, in Fig. 2g we see that 16 ions appear to lie on 3 rings. The larger ring, containing 8 ions, lies near the x-y plane and the smaller rings, each containing 4 ions, lie in planes above and below but parallel to the x-y plane. We may also view these ions as lying on the surface of a spheroidal shell characteristic of the structure for large numbers of ions.[16-18] In principle, it should be possible to observe ordered structures of much larger numbers of atomic ions in rf traps. In our trap, this was difficult for $N_i \gtrsim 20$ because the small amount of power available for cooling was unable to overcome the rf heating.[19] In rf heating, the kinetic energy of the ion's driven motion (at the trapping field frequency) is coupled into the secular motion characteristic of the pseudopotential well.

3. SHELL STRUCTURE PHASE IN A PENNING TRAP ($\leq$ 15 000 IONS)

In Penning traps,[14] where ions are confined by static electric and magnetic fields, rf heating does not take place and large collections of ions can be cooled to temperatures less than 10 mK. This larger system is closer to the conditions of an infinite volume plasma and should display a rich variety of phenomena.

The boundary conditions are still expected to have a significant effect on the state of a finite plasma consisting of a hundred to a few thousand ions. Molecular-dynamics simulations involving these numbers of ions have been done for the conditions of a spherical[16-18] and spheroidal[20,21] trap potential. Instead of a sharp phase transition to a bcc lattice, the simulations predict that the plasma will separate into concentric, nearly spheroidal shells (due to the shape of the trap potential) which gradually become more pronounced as Γ increases. These shells are one ion thick, and the distance between ions on the surface of a shell is predicted to be approximately equal to the shell separation. Another interesting prediction is that there should be a range of conditions where the ions will behave like a liquid within a shell (short range order with diffusion) and a solid across shells (no diffusion between shells).[18] This characteristic is similar to some phases of smectic liquid

crystals.[22] At higher Γ a distorted 2D hexagonal lattice is expected to form on the outer shells.[18]

We have investigated this system using $^9Be^+$ ions trapped in the cylindrical Penning trap shown schematically in Fig. 3. A magnetic field $\vec{B} = B\hat{z}$ ($B = 1.92$ T) produced by a superconducting magnet confined the ions in the direction perpendicular to the z axis. A static potential V_o between the end and central cylinders confined the ions in the z direction to a region near the center of the trap. The dimensions of the trap electrodes were chosen so that the first anharmonic term of the trapping potential was zero. Over the region near the trap center, the electric field potential can be expressed (in cylindrical coordinates) as $\Phi \cong AV_o(2z^2 - r^2)$, where $A = 0.146$ cm^{-2}. This potential, when combined with the magnetic field, forces the cloud into a spheroidal shape.[2,3] The ions' thermal distribution is superimposed on a uniform rotation of the cloud[1-3] (frequency ω) due to $\vec{E}x\vec{B}$ drift, where $\vec{E}$ is the electric field due to the trap voltage and the space charge of the ions.

The ions were laser cooled and optically pumped into the $2s\ ^2S_{1/2}(M_I=3/2,M_J=1/2)$ state by driving the $2s\ ^2S_{1/2}(3/2,1/2) \rightarrow 2p\ ^2P_{3/2}(3/2,3/2)$ transition slightly below the resonant frequency.[2,3] The 313 nm cooling radiation (≈ 30 μW) could be directed perpendicular to the magnetic field and/or along a diagonal as indicated in Fig. 3. In addition to cooling the ions, the laser also applied an overall torque which would either compress or expand the cloud.[2,3] We controlled the size of the cloud by choosing the radial positions (and thus the torques) of the perpendicular and diagonal beams.

About 0.04% of the 313 nm fluorescence from the decay of the $^2P_{3/2}$ state was focused by f/10 optics onto the photocathode of the same imaging tube used in the Hg^+ experiments. The imager was located along the z axis, about 1 m from the ions. The imaging optics was composed of a three stage lens system with overall magnification of 27 and a resolution limit (FWHM) of about 5 μm. Count rates ranged from 2 to 15 kHz.

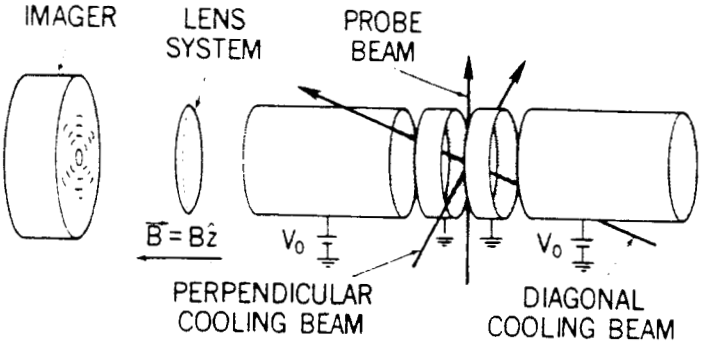

Fig. 3 Schematic drawing of the trap electrodes, laser beams, and imaging system (not to scale) for the Penning trap experiment. The overall length of the trap is 10.2 cm. The trap consists of two end cylinders and two electrically connected central cylinders with 2.5 cm inner diameters. Ion clouds are typically less than 1 mm both in diameter and axial length. The diagonal cooling beam crosses the cloud at an angle of 51° with respect to the z axis.

A second laser (power ≈ 1 μW, beam waist ≈ 30 μm) was used to spatially map the shell structure of the cloud. This probe laser was tuned to the same transition as the cooling laser and was directed through the cloud perpendicularly to the magnetic field. With the probe laser on continuously, the cooling laser could be chopped at 1 kHz and the image signal integrated only when the cooling laser was off. Different portions of the cloud could be imaged by translating the probe beam, in a calibrated fashion, either parallel or perpendicular to the z axis. Images were also obtained from the ion fluorescence of all three laser beams.

The probe beam was also used to measure the cloud rotation frequency ω and the ion temperature. For these measurements, the probe laser was tuned to a transition which optically pumped the ions out of the $^2S_{1/2}(3/2,1/2)$ level.[2,3] This resulted in a decrease in the fluorescence from the cooling laser beams as the probe laser was scanned through the "depopulation" transition. We determined ω by measuring the change in the Doppler shift of the depopulation signal as the probe beam was translated perpendicularly to the z axis. The density n_o could then be calculated[1,2] from $n_o = m\omega(\Omega - \omega)/(2\pi q^2)$

where $\Omega = qB/mc$ is the cyclotron frequency. With the use of n_o and the cloud size obtained from probe beam images, the total number of ions was calculated. The ion temperature was derived from the Doppler broadening contribution to the spectral width of the depopulation signal.[2,3] From the measured values of the temperature and the density, Γ was calculated using Eq. (1).

We have observed shell structure in clouds containing as few as 20 ions (1 shell) and in clouds containing up to about 15 000 ions (16 shells).[7] Images covering this range are shown in Fig. 4. We measured the coupling constant Γ for several clouds containing about 1000 ions. Possible drifts in the system parameters were checked by verifying that the same images were obtained before and after the cloud rotation frequency and ion temperatures were measured.

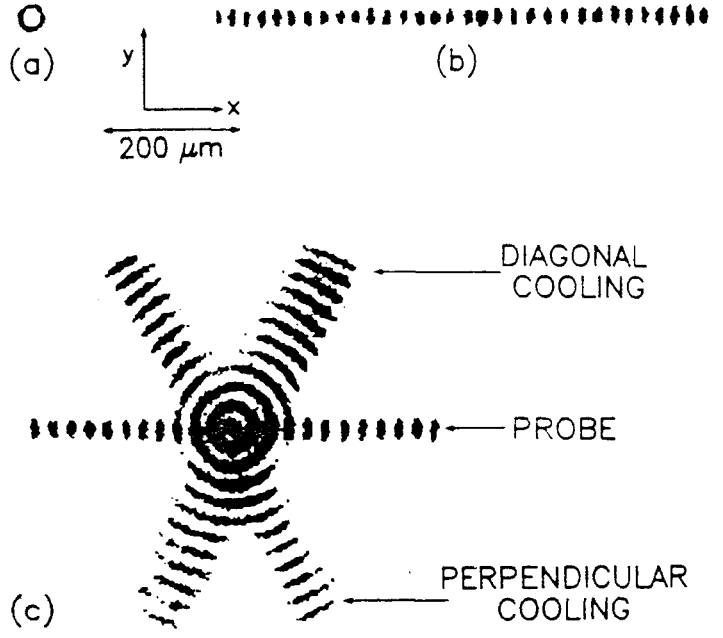

Fig. 4 Images of shell structures. (a) A single shell in a cloud containing approximately 20 ions. (b) Sixteen shells (probe beam ion fluorescence only) in a cloud containing about 15 000 ions. (c) Eleven shells plus a center column in the same cloud as (b), with lower trap voltage. This image shows the ion fluorescence from all three laser beams. Integration times were about 100 seconds.

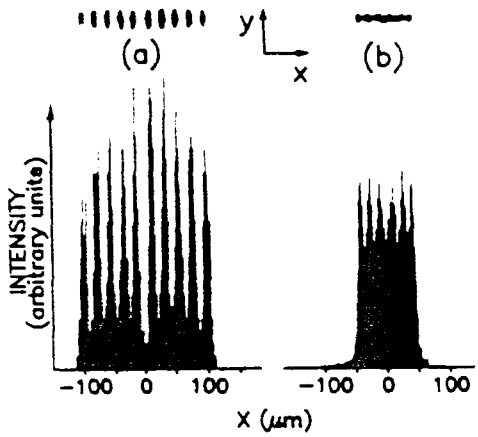

Fig. 5 Intensity plots along the x axis through the center of the ion cloud with corresponding probe beam images (above). (a) $\Gamma = 180^{+90}_{-30}$ ($T = 6^{+4}_{-2}$ mK, $n_0 \approx 7 \times 10^7$ ions cm^{-3}). (b) $\Gamma = 50^{+20}_{-20}$ ($T = 33^{+17}_{-13}$ mK, $n_0 = 2 \times 10^8$ ions cm^{-3}). The clouds contained about 1000 ions in both cases.

Figure 5 shows examples of shell structures at two different values of Γ. The first image is an example of high coupling ($\Gamma \approx 180$) showing very good shell definition in an intensity plot across the cloud. The second image is an example of lower coupling ($\Gamma \approx 50$) and was obtained by only cooling perpendicular to the magnetic field. Variations in peak intensities equidistant from the z axis are due to signal-to-noise limitations and imperfect alignment between the x axis and the probe beam.

We obtained three dimensional information on the shell structure by moving the probe beam to obtain images at different z positions. We found that there were two types of shell structure present under different circumstances. The first type showed shell curvature near the ends of the cloud, indicating that the shells may have been closed spheroids. Shell closure was difficult to verify due to lack of sharp images near the ends of the cloud where the curvature was greatest. This was, in part, due to the averaging of the shells over the axial width of the probe beam. In the other type of shell structure, it was clear that the shells were concentric cylinders

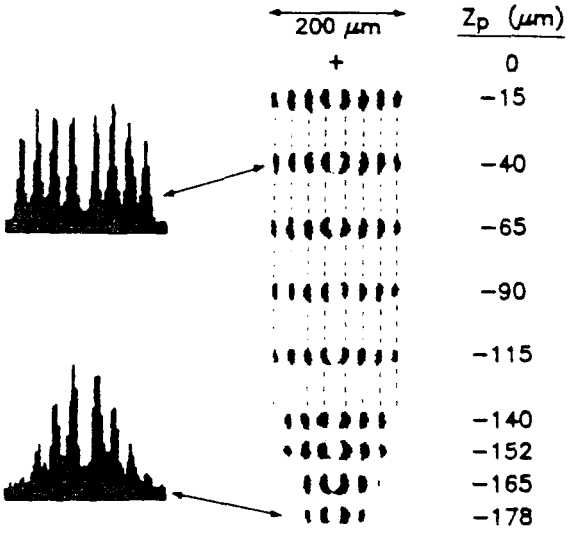

Fig. 6 Data showing evidence for concentric cylindrical shells. On the right is a series of images obtained with the probe beam for different z positions z_p of the probe beam (lower half of the cloud only). Intensity plots for z_p = -40 μm and z_p = -178 μm are shown on the left. The cloud axial length/diameter ratio was about 1.9.

with progressively longer cylinders near the center. An example of these data is shown in Fig. 6. Other evidence for cylindrical shells can be obtained from the fact that shells in the diagonal beam images occur at the same cylindrical radii as those from the perpendicular beams. This can be seen in the three-beam images such as that shown in Fig. 4(c). Systematic causes of these two different shell configurations have not yet been identified.

So far, our discussion has been limited to the static structure of strongly coupled ion clouds. Other experiments have provided dynamical information. For example, ions can be switched off (removed from the cooling cycle) by driving the probe depopulation transition. With appropriate positioning of this depopulating laser beam, certain parts of the ion cloud were tagged, allowing ion diffusion studies through the movement (or lack of movement) of the tagged ions. In this way we have recently distinguished the relatively rapid diffusion (≥ 100 μm/0.1 s) of ions within a shell

from the much slower diffusion (several seconds) between shells, verifying the smectic nature of this interesting form of matter. We plan to do more detailed diffusion studies in the near future.

At present, it is difficult to make many quantitative comparisons between our data and the simulations. There is substantial uncertainty in our measurement of Γ due to uncertainty in the temperature measurement. Also, the spatial resolution is partially limited by the optics. One comparison which can be made, however, is the relationship between the number of shells and the number of ions, N_i, in a cloud. For a spherical cloud, approximately $(N_i/4)^{1/3}$ shells are predicted.[16] For the nearly spherical cloud of Fig. 4(b) ($N_i \approx 15\,000$) this formula predicts 15.5 shells and we measured 16.

Our data do agree qualitatively with the simulations with the exception of the observation of open cylinder shell structures as opposed to the predicted closed spheroids.[16-18,20,21] It is possible that shear (that is, different rotation frequencies) between the shells may account for this discrepancy.[20] In our experiment, shear could be caused by differential laser torque or the presence of impurity ions.[23] For the data here, we have determined that the rotation frequency does not vary by more than 30% across the cloud. This is comparable to the limits discussed in Refs. 3 and 23.

4. FUTURE EXPERIMENTS

A number of future experiments will allow us to better understand strong coupling in ion clouds. In the near future, we expect to have better light collection optics which will yield improved spatial resolution and collection solid angle for the Penning trap experiment. With these optics we will be able to obtain more quantitative data on the ion diffusion times and see how the diffusion varies with Γ. Also, spectrum analysis of the scattered light from strongly coupled ions can possibly be used to study mode structure of ordered ion motion. Both of these studies may be aided by the use of sympathetic cooling[23] whereby two ion species are

confined simultaneously in the same trap. One ion species is laser cooled and by Coulomb interaction cools and maintains the second ion species at constant temperature. Dynamical studies are then performed on the second ion species.

Increasing the cooling power in the experiments should allow larger ($N_i >> 10^5$) samples of ions to be cooled. This may permit the observation of structure characteristic of the infinite volume regime in which a body-centered cubic (bcc) lattice is predicted.[8] Detailed images in the Penning traps are made difficult by the rotation of the cloud which averages over azimuthal angle. In principle, it should be possible to strobe the laser or detection electronics at a frequency harmonically related to ω, but this requires ω to be sufficiently stable. Fluctuations in ion density may make this difficult but perhaps a single strongly fluorescing ion (such as Mg^+) which is locked onto the rotating lattice (of Be^+) could serve as a "beacon" and aid in determining ω. Another possible technique for observation of bcc structure is Bragg scattering.[2,3] Also, intensity correlation functions which are a function of x-y position[24] may allow us to extract spatial correlation information.

At present, the rather large uncertainty in Γ in the Penning trap experiments comes from the uncertainty in our measurement of temperature. This is so because the Doppler broadening contribution of the optical spectrum is small compared to the radiative, or natural broadening. This limitation can be overcome by driving transitions whose radiative broadening is negligible as in the Hg^+ experiments.[5,25] For Be^+ and Mg^+ ions, two-photon stimulated Raman transitions might be used for this purpose.[2]

Finally, it would be very useful to study large numbers of particles in a rf trap. One clear advantage over a Penning trap is that ions can remain fixed without rotation. For large numbers of ions, the mechanism of rf heating must be overcome. This may be aided by using higher laser cooling power, smaller ratios of secular to drive frequencies, and insuring that impurity ions are absent.

Acknowledgements

We gratefully acknowledge support from the Office of Naval Research and the Air Force Office of Scientific Research. We also thank C.E. Wieman and C.S. Weimer for helpful suggestions on the manuscript.

REFERENCES

1. J.H. Malmberg and T.M. O'Neil, Phys. Rev. Lett. 39, 1333 (1977).

2. J.J. Bollinger and D.J. Wineland, Phys. Rev. Lett. 53, 348 (1984); L.R. Brewer, J.D. Prestage, J.J. Bollinger, and D.J. Wineland, in Strongly Coupled Plasma Physics, edited by F.J. Rogers and H.E. Dewitt (Plenum, New York, 1987), p. 53.

3. L.R. Brewer, J.D. Prestage, J.J. Bollinger, W.M. Itano, D.J. Larson, and D.J. Wineland, Phys. Rev. A., in press.

4. J.H. Malmberg, T.M. O'Neil, A.W. Hyatt, and C.F. Driscoll, in Proceedings of the 1984 Sendai Symposium on Plasma Nonlinear Phenomena, edited by N. Sato (Tohoku University, Sendai, Japan, 1984), p. 31.

5. D.J. Wineland, J.C. Bergquist, W.M. Itano, J.J. Bollinger, and C.H. Manney, Phys. Rev. Lett. 59, 2935 (1987).

6. F. Diedrich, E. Peik, J.M. Chen, W. Quint, and H. Walther, Phys. Rev. Lett. 59, 2931 (1987).

7. S.L. Gilbert, J.J. Bollinger, and D.J. Wineland, Phys. Rev. Lett. 60, 2022 (1988).

8. S. Ichimaru, H. Iyetomi, and S. Tanaka, Phys. Rep. 149, 91 (1987) and references therein.

9. R.F. Wuerker, H. Shelton, and R.V. Langmuir, J. Appl. Phys. 30, 342 (1959); D.J. Wineland, W.M. Itano, J.C. Bergquist, S.L. Gilbert, J.J. Bollinger, and F. Ascarrunz, in Nonneutral Plasma Physics, edited by C.W. Roberson, Am. Inst. Phys. Conf. Series, 1988, to be published.

10. See for example: A.J. Dahm and W.F. Vinen, Physics Today 40, 43 (Feb., 1987).

11. D.J. Aastuen, N.A. Clark, and L.K. Cotter, Phys. Rev. Lett. 57, 1733 (1986); J.M. di Meglio, D.A. Weitz, and P.M. Chaikin, Phys. Rev. Lett. 58, 136 (1987); C.A. Murray and D.H. Van Winkle, Phys. Rev. Lett. 58, 1200 (1987).

12. J.P. Schiffer and O. Poulsen, Europhys. Lett. 1, 55 (1986); D. Habs, in Lecture Notes in Physics 296, edited by M. Month and S. Turner, (Springer-Verlag, Berlin, 1988), p. 310.

13. J.C. Bergquist, D.J. Wineland, W.M. Itano, H. Hemmati, H.U. Daniel, and G. Leuchs, Phys. Rev. Lett. 55, 1567 (1985).

14. See for example: H.G. Dehmelt, Adv. At. Mol. Phys. 3, 53 (1967) and 5, 109 (1969); D.J. Wineland, W.M. Itano, and R.S. Van Dyck, Jr., Adv. At. Mol. Phys. 19, 135 (1983).

15. W.M. Itano et. al., to be published; our simulations agree with independent ones of D.H.E. Dubin (performed on up to 10 ions).

16. A. Rahman and J.P. Schiffer, Phys. Rev. Lett. 57, 1133 (1986); J.P. Schiffer, submitted for publication.

17. H. Totsuji, in Strongly Coupled Plasma Physics, edited by F.J. Rogers and H.E. Dewitt (Plenum, New York, 1987), p. 19.

18. D.H.E. Dubin and T.M. O'Neil, Phys. Rev. Lett. 60, 511 (1988).

19. D.A. Church and H.G. Dehmelt, J. Appl. Phys. 40, 3421 (1969); H.G. Dehmelt, in Advances in Laser Spectroscopy, edited by F.T. Arecchi, F. Strumia, and H. Walther (Plenum, New York, 1983), p. 153.

J.P. Schiffer, Physics Dept., Univ. of Chicago, Chicago, IL, private communication.

D.H.E. Dubin, Physics Dept., Univ. of California - San Diego, La Jolla, CA, private communication.

P.G. de Gennes, The Physics of Liquid Crystals, (Oxford University Press, London, 1974).

D.J. Larson, J.C. Bergquist, J.J. Bollinger, W.M. Itano, and D.J. Wineland, Phys. Rev. Lett. 57, 70 (1986).

N.A. Clark, B.J. Ackerson, and A. J. Hurd, Phys. Rev. Lett. 50, 1459 (1983).

J.C. Bergquist, W.M. Itano, and D.J. Wineland, Phys. Rev. A36, 428 (1987).